Response of alpha particles in hexagonal boron nitride neutron detectors

T. C. Doan, J. Li, J. Y. Lin, and H. X. Jiang[a)]
Department of Electrical and Computer Engineering, Texas Tech University, Lubbock, Texas 79409, USA

(Received 23 February 2017; accepted 12 May 2017; published online 24 May 2017)

Thermal neutron detectors were fabricated from ^{10}B enriched h-BN epilayers of different thicknesses. The charge carrier generation and energy loss mechanisms as well as the range of alpha daughter particles generated by the nuclear reaction between thermal neutrons and ^{10}B atoms in hexagonal boron nitride (h-BN) thermal neutron detectors have been investigated via their responses to alpha particles from a ^{210}Po source. The ranges of alpha particles in h-BN were found to be anisotropic, which increase with the angle (θ) between the trajectory of the alpha particles and c-axis of the h-BN epilayer following $(\cos\theta)^{-1}$ and are 4.6 and 5.6 μm, respectively, for the alpha particles with energies of 1.47 MeV and 1.78 MeV at $\theta = 0$. However, the energy loss of an alpha particle inside h-BN is determined by the number of layers it passes through with a constant energy loss rate of 107 eV per layer due to the layered structure of h-BN. Roughly 5 electron-hole pairs are generated when an alpha particle passes through each layer. It was also shown that the durability of h-BN thermal neutron detectors is excellent based on the calculation of boron vacancies generated (or ^{10}B atoms consumed) by neutron absorption. The results obtained here provide useful insights into the mechanisms of energy loss and charge carrier generation inside h-BN detectors and possible approaches to further improve the overall performance of h-BN thermal neutron detectors, as well as the ultimate spatial resolution of future neutron imaging devices or cameras based on h-BN epilayers. *Published by AIP Publishing*. [http://dx.doi.org/10.1063/1.4984112]

Thermal neutron detectors based on hexagonal boron nitride (h-BN) epilayers have demonstrated to date the highest detection efficiency of 51.4% among solid-state detectors.[1,2] Currently, the most deployed detectors for detecting fissile materials are ^{3}He gas detectors. However, not only are ^{3}He gas detectors bulky, hard to configure, and require high voltage operation but also there is a worldwide shortage of ^{3}He gas. Thus, there has been a continuing effort to develop solid-state neutron detectors that have the performance approaching that of ^{3}He gas detectors without their drawbacks.[1–9] Potential applications of solid-state neutron detectors are numerous and include fissile materials sensing for security, neutron therapy for medical imaging, and neutron scattering and imaging for material and protein structure exploration.[1–9]

The working principle of BN thermal neutron detectors is based on the fact that the boron-10 (^{10}B) isotope has a large capture cross-section of 3840 barns for thermal neutrons.[10,11] When a ^{10}B atom captures a neutron, it undergoes the following nuclear reaction

$$^{10}_{5}B + {}^{1}_{0}n = {}^{7}_{3}Li^{*}\,(0.84\,MeV) + {}^{4}_{2}\alpha^{*}(1.47\,MeV) \times [94\%\ excited\ state] \quad (1a)$$

$$^{10}_{5}B + {}^{1}_{0}n = {}^{7}_{3}Li\,(1.015\,MeV) + {}^{4}_{2}\,\alpha\,(1.777\,MeV) \times [6\%\ ground\ state] \quad (1b)$$

$$\mathrm{Li}, \alpha \rightarrow \mathrm{N}\,(\mathrm{e}^{-}) + \mathrm{N}\,(\mathrm{h}^{+}). \quad \mathrm{N} \sim 10^{5}. \quad (2)$$

The detection of neutrons by an h-BN detector is accomplished by two sequential processes. The first is the neutron capture of Eq. (1) in which the nuclear reaction creates Li and α daughter particles with large kinetic energies. The second process of Eq. (2) is the subsequent charge carrier generation by Li and α particles and electron (e^-) and hole (h^+) collection, which resembles the process in a semiconductor alpha particle detector. In BN detectors, the two sequential processes described in Eqs. (1) and (2) occur in the same BN layer, making high detection efficiency possible. Moreover, BN detectors possess a negligible response to γ-photons because BN is composed of low atomic number elements.[1,12–15] Furthermore, freestanding h-BN epilayers are flexible, enabling the possibility for constructing detectors with versatile form factors.[1]

To obtain h-BN detectors with enhanced performance, an improved understanding of the energy loss and charge carrier generation processes in h-BN is highly desirable. However, until now, the thermal neutron detection processes in h-BN detectors have been studied through neutron count rates or pulse height spectra in response to a thermal neutron source,[1,12–15] in which the two processes described in Eqs. (1) and (2) are coupled. To gain an in-depth understanding of the mechanisms of charge carrier generation and energy loss in h-BN detectors, it is desirable to decouple these two processes. As a semiconductor material, h-BN epilayers are also a good candidate for the fabrication of neutron imaging devices or cameras with the potential of providing a much higher spatial resolution than the current state of the art. Ultimately, the spatial resolution will be determined by the range of α particles in h-BN epilayers. Although a range of 5 μm (2 μm) for α (Li) daughter particles in pyrolytic h-BN has been reported,[3] a more complete study which accounts for the anisotropic structure of h-BN is needed.

In this work, the mechanisms of energy loss and charge carrier generation in h-BN have been investigated by employing h-BN as alpha particle detectors so that the

a)hx.jiang@ttu.edu

processes of neutron capture and charge carrier generation are decoupled. Boron-10 (^{10}B) enriched h-BN epilayers of different thicknesses up to 4.5 μm were synthesized by metal organic chemical vapor deposition (MOCVD) and the details of epilayer growth processes have been described previously.[1,11–15] Figure 1(a) shows a schematic structure of ^{10}B enriched h-BN epilayers used in this work. Thermal neutron detectors based on a metal-semiconductor-metal (MSM) architecture with micro-strip interdigital fingers were fabricated. Figures 1(b) and 1(c) are micrographs of a representative h-BN MSM detector with a thickness of 2.7 μm. Interdigital finger patterns consisting of micro-strips with 15 μm (width)/3 μm (spacing) were etched all the way to the sapphire substrate by a modified drying etching process established for GaN.[16,17] Metal contacts consisting of bilayers of Ti/Al (20 nm/30 nm) as well as the bonding pads (200 nm of Au) were deposited by e-beam evaporation.[12–15]

A ^{210}Po alpha source with a peak energy of 5.31 MeV was used to supply alpha particles. The ^{210}Po source was covered by a thick metal film containing a small hole in the middle to provide a collimated alpha particle beam. A neutron source of ^{252}Cf with a radioactivity of 4.0×10^6 neutrons/s moderated by 1-in. thick high density polyethylene (HDPE) block was also used to convert fast neutrons to thermal neutrons.[11] Detection electronics were obtained from Cremat Inc. and have been described in elsewhere.[1,11–13] The detector package is light-tight. Experiment was set up in such a way that the distance between the detector and alpha (neutron) source was 1.1 (30) cm. Pulse height spectra of alpha (neutron) responses were recorded at a bias voltage of 50 (400) V for 1 (10) min. The corresponding "dark" response was measured in the absence of any radiation exposure under the same conditions.

Figure 2(a) shows the I-V characteristics of a representative 2.7 μm thick detector measured in a bias voltage range between −100 and 100 V under dark and alpha particle irradiation, which clearly revealed an increase in current due to charge carrier generation by alpha particles. Moreover, the results also show that the alpha-current increases with an increase in the bias voltage under a constant alpha particle flux. In a semiconductor detector, the presence of deep level defects with sufficiently high concentrations will induce effects of charge trapping and persistent photoconductivity (or alpha-conductivity in this case),[18] meaning that the photo-current (or alpha-current) cannot decay to the dark level hours or even days after the termination of the excitation source. Therefore, measuring the decay kinetics of photo-current (or alpha-current) is an effective way to gauge the effect of deep level defects. Figure 2(b) plots the alpha-current kinetics, revealing that the response of the detector to the alpha particle source is very fast. The results are an indicative that deep level traps in h-BN epilayers have a

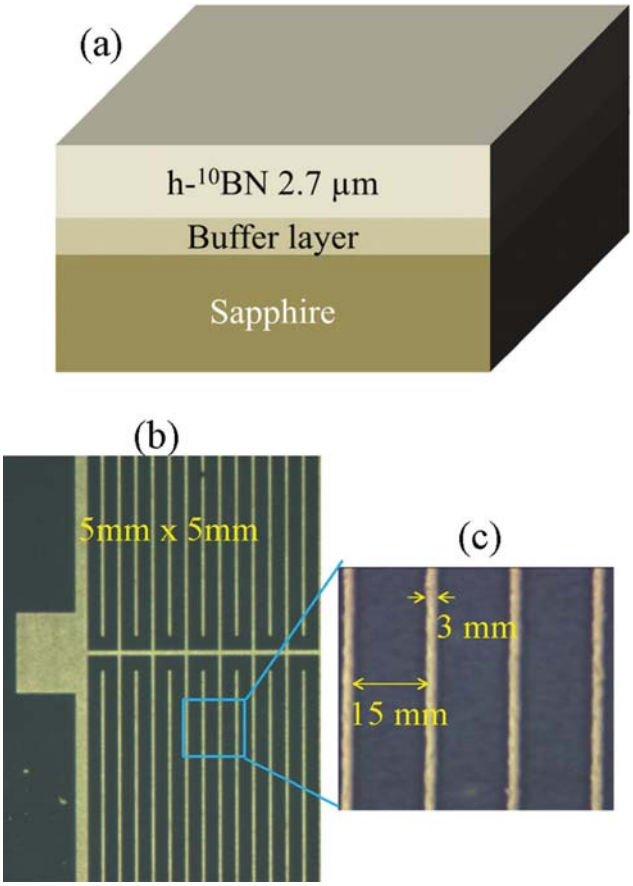

FIG. 1. (a) Schematic structure of ^{10}B enriched h-BN epilayers used in this study. (b) and (c) Micrographs of a representative ^{10}B enriched h-BN MSM detector with a dimension of 5 mm × 5 mm and widths of etched trenches and micro-strips of 3 μm and 15 μm, respectively.

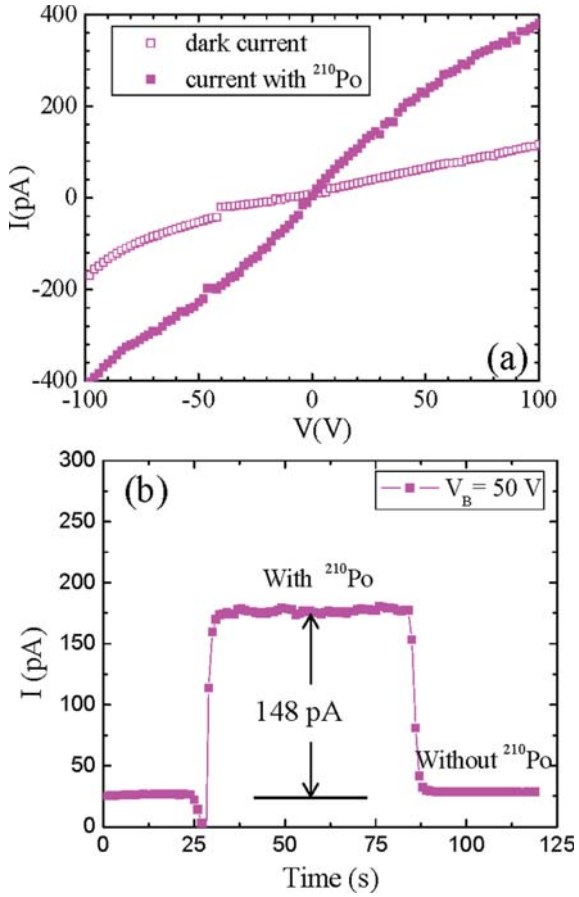

FIG. 2. (a) I-V characteristics of a representative detector of 2.7 μm in thickness measured in "dark" and under irradiation of a ^{210}Po alpha particle source with an energy of 5.31 MeV. (b) Response kinetics of current generated by alpha particles from a ^{210}Po source with an energy of 5.31 MeV.

negligible effect on the charge carrier generation and collection.

Schematic diagrams of the experimental setup for measuring the pulse height spectra of ^{10}B enriched h-BN detectors in response to the ^{210}Po alpha source are shown in Fig. 3. When the alpha particles move along the c-axis, as illustrated in Fig. 3(a), the energy of alpha particles passing through the h-BN layer with a thickness d can be expressed by

$$E(d) = E_0 - \kappa d, \tag{3}$$

where κ describes the energy loss of alpha particles passing through a unit length. Figure 4 shows the pulse height spectra of h-BN detectors with different thicknesses measured in the configuration of Fig. 3(a). A peak is clearly observed in each pulse height spectrum. The higher the energy deposited in h-BN, the more electrons and holes are generated and consequently the higher the energy peak position in the pulse height spectrum. Therefore, the peak position moves towards higher energies as the layer thickness of the detector increases. The pulse height spectrum of the 2.7 μm thick detector in response to the thermal neutron source is also included in Fig. 4(a) as a reference, where the sum peak at 2.31 MeV resulting from the nuclear reaction of Eq. (1a) with a 94% probability is very prominent.

It is interesting to note that all peaks appear at the highest energy positions in the pulse height spectra in response to α particles. If the concentration of impurities/defects is sufficiently high in h-BN detectors, a fraction of charge carriers generated by alpha particles will be trapped by defects. The lost carriers will manifest themselves as counts appearing below the peak position in the corresponding pulse height spectrum. As we can see that each pulse height spectrum shown in Fig. 4 exhibits only one clear peak at the highest energy position. The results are an indication that that the charge collection efficiency of h-BN detectors is very high, i.e., the maximum number of charge carriers collected is almost equal to the maximum number of charge carriers generated inside h-BN. The results shown in Fig. 4 corroborate the rapid alpha-current response shown in Fig. 2 and are also consistent with the previously demonstrated high charge collection efficiency of 86.1% for h-BN neutron detectors.[1] Figure 4(e) plots the peak position of the pulse height spectra of h-BN detectors in response to alpha particles as a function of the detector's layer thickness (d). The variation of the peak position with d can be described very well by Eq. (3). The intercept in the y-axis at d = 0 (0.85 MeV) corresponds to the energy loss of alpha particles from the ^{210}Po source having an energy loss rate of 0.75 MeV/cm in air[9] and is consistent with the fact that the ^{210}Po source is located at 1.1 cm away from the front surface of the h-BN detectors. The slope of the line represents the energy loss of alpha particles inside h-BN detectors, which is 0.32 MeV/μm. Since the interlayer distance in h-BN is 3.33 Å or 3000 layers/μm as illustrated in Fig. 3(b), this corresponds to an energy loss of about 107 eV per layer. It is also known that the amount of energy, E_a, required to generate an electron-hole pair in a semiconductor with an energy bandgap E_g is E_a=3E_g,[19] which is around

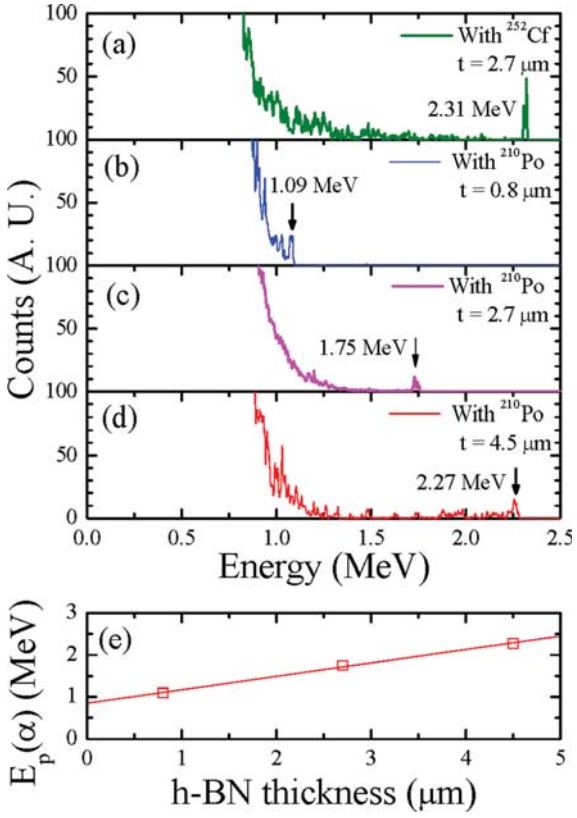

FIG. 4. Pulse height spectra of h-BN detectors of different thicknesses in response (a) to a thermal neutron source as a reference; (b)–(d) to an alpha particle source of ^{210}Po. (e) The peak position of pulse height spectra of h-BN detectors in response to an alpha source of ^{210}Po as a function of detector layer thickness.

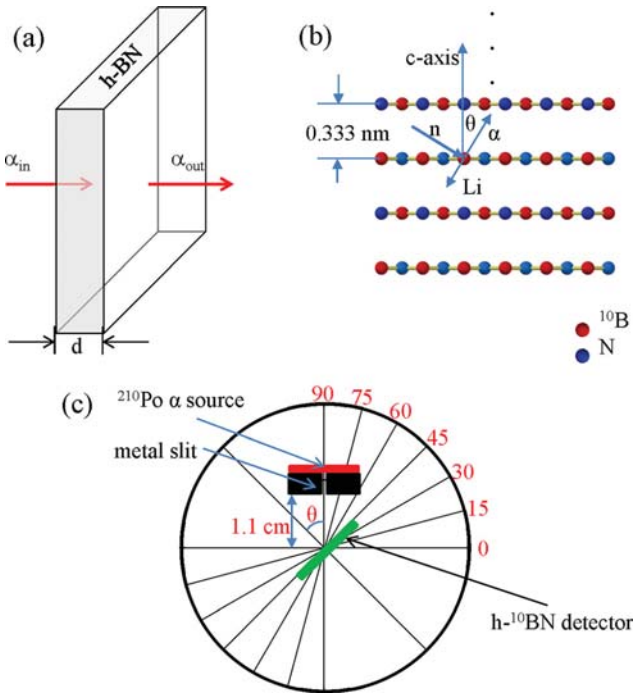

FIG. 3. Schematic diagrams of (a) set up for measuring the pulse height spectra of ^{10}B enriched h-BN detectors using an alpha source of ^{210}Po with an energy of 5.31 MeV; (b) nuclear reaction of Eq. (1) and trajectory of α and Li daughter particles; and (c) set up for measuring the angle dependence of pulse height spectra of the h-BN detector in response to a ^{210}Po α source with an energy of 5.31 MeV.

20 eV in h-BN with E_g=6.5 eV. This means that on average 5 electron-hole pairs are generated when an alpha particle passing through each layer.

As a neutron detector, based on the dominant nuclear reaction described by Eq. (1), each absorbed neutron is expected to generate an alpha particle with a kinetic energy of 1.47 MeV (94% probability) or 1.78 MeV (6% probability). The energy loss mechanism of daughter alpha particles can thus be understood based on the results shown in Fig. 4. For the nuclear reaction generating 1.47 (1.78) MeV with 94% (6%) chance, if an alpha particle moves along the c-axis of h-BN, it will pass through a total of $d_r(\theta = 0)$=1.47 (1.78) MeV/(0.32 MeV/μm)=4.6 (5.6) μm before it loses all its energy. The results thus provide a range in h-BN of 4.6 and 5.6 μm for the alpha particles with energies of 1.47 MeV and 1.78 MeV, respectively. These results are consistent with an early reported range of about 5 μm for the alpha daughter particles in pyrolytic h-BN.[3] However, the derived range is inadequate when the alpha particles move in directions other than the c-axis.

To understand the processes in more general scenarios, we measured pulse height spectra of the representative 2.7 μm thick h-BN detector for varying incident angles (θ) of the incoming alpha particle beam relative to the c-axis of h-BN, as illustrated schematically in Figs. 3(b) and 3(c). The path length of an alpha particle inside h-BN increases with an increase of θ. However, the pulse height spectra obtained at varying angles (θ) shown in Fig. 5 revealed that the peak positions of the pulsed height spectra are independent of θ. This points to the fact that the energy loss of an alpha particle is determined only by the number of layers it passes through. This is understandable by realizing that h-BN is a layer structured material. With the above interpretation, the mechanism of energy loss of α daughter particles generated by the nuclear reaction of Eq. (1) can be understood. The range of these alpha particles depends on the angle θ, as shown in Fig. 3(b) according to

$$d_r(\theta) = d_r(\theta = 0)/\cos\theta\,(0 \le \theta \le \theta_{max} < 90^\circ), \quad (4)$$

where $d_r(\theta = 0)$ is the range of alpha daughter particles along the c-axis of h-BN, $\theta = 0$. The condition of $\theta \le \theta_{max} < 90^\circ$ accounts for the fact that the nearest-neighbor N atoms surrounding the ^{10}B atom involved in the nuclear reaction of Eq. (1) has a certain size and the angle of the alpha particle generated by the nuclear reaction must be smaller than 90° in order to travel inside h-BN.

Another relevant issue is the durability of h-BN neutron detectors. In the absence of any radiation, the variation of h-BN detector performance with time can be neglected due to the inherent stability of h-BN in air. Instead, we concentrate on the ability of h-BN detectors for detecting thermal neutrons by considering the fact that B atoms inside h-BN are being consumed by thermal neutron irradiation. We will apply the general rule of thumb that the performance of a semiconductor device would not be affected if the impurity or defect concentration is below 10^{13} cm^{-3}, while the typical doping concentration needed to control the conductivity of a semiconductor is greater than 10^{16} cm^{-3}. The nuclear reaction described by Eq. (1) indicates that a B atom is consumed after absorbing a thermal neutron and consequently a B vacancy (V_B) is created in h-BN. Assuming a thermal neutron flux of 5 n/cm^2·s on the detector side, a detector with an area of A and a thickness of 50 μm corresponding to a neutron absorption probability of 65% and a charge collection efficiency of 85%,[1] the detector will provide a count rate of around 2.8 counts/s. The generation rate of V_B concentration, N[V_B], in the h-BN detector will be around 5/s·cm^2 × A × 65% × 85%/(A × 50 × 10^{-4} cm)=5.5 × 10^2/cm^3·s, which is very small. For security applications, detecting neutrons is a rare event and the concentration of V_B, N[V_B], generated by absorption of neutrons is really insignificant. For other applications, such as for continuous neutron flux monitoring, assuming the same thermal neutron flux, the concentration of V_B, N[V_B], generated with continuing counting for 1 year (3.15×10^8 s) would be 3.15×10^8 s × 5.5 × 10^2/cm^3·s = 1.7×10^{11} cm^{-3}. This concentration is still 2 orders of magnitude smaller than 10^{13} cm^{-3}. It is clear from the above argument that V_B generation through neutron absorption will not affect the performance of h-BN neutron detectors.

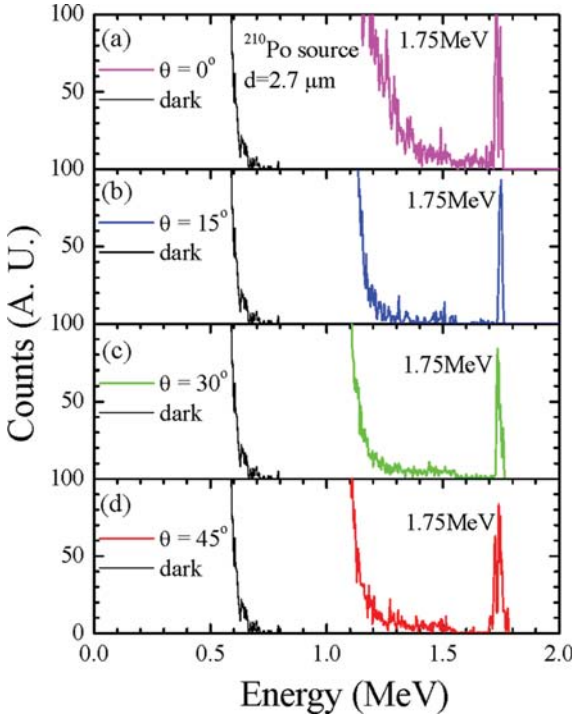

FIG. 5. Pulse height spectra of h-BN detectors of a representative 2.7 μm thick detector obtained at different incoming α particle beam angles relative to the c-axis of h-BN.

In summary, the responses of α particles in h-BN thermal neutron detectors have been investigated. It was found that the range of α particles inside h-BN is anisotropic and is around 5 μm when they travel in the direction along the c-axis ($\theta = 0$) and increases with the angle (θ) between the trajectory of the α particle and c-axis of h-BN epilayer according to $(\cos\theta)^{-1}$. The energy loss of an α particle in h-BN can be described simply by the number of layers through which the α particle passes through at a rate of 107 eV per layer. Roughly 5 electrons and holes are generated as an α particle crossing over each layer in h-BN.

We would like to acknowledge the support by the DOE NNSA SSAA program (DE-NA0002927) for the neutron detector work. The study of the basic structural properties of *h*-BN was supported by the NSF (ECCS-1402886). Jiang and Lin are grateful to the AT&T Foundation for the support of Ed Whitacre and Linda Whitacre Endowed chairs.

[1]A. Maity, T. C. Doan, J. Li, J. Y. Lin, and H. X. Jiang, Appl. Phys. Lett. **109**, 072101 (2016).
[2]See AIP Journals in the News https://publishing.aip.org/publishing/journal-highlights/hexagonal-boron-nitride-semiconductors-enable-cost-effective-detection for information about "Hexagonal Boron Nitride Semiconductors Enable Cost-Effective Detection of Neutron Signals."
[3]F. P. Doty, "Boron nitride solid-state neutron detector," U.S. patent 6,727,504 (2004).
[4]D. S. McGregor and J. K. Shultis, Nucl. Instrum. Methods Phys. Res., A **517**, 180 (2004).
[5]R. T. Kouzes, J. H. Ely, L. E. Erikson, W. J. Kernan, A. T. Lintereur, E. R. Siciliano, D. L. Stephens, D. C. Stromswold, R. M. Van Ginhoven, and M. L. Woodring, Nucl. Instrum. Methods. Phys. Res., A **623**, 1035 (2010).
[6]Q. Shao, L. F. Voss, A. M. Conway, R. J. Nikolic, M. A. Dar, and C. L. Cheung, Appl. Phys. Lett. **102**, 063505 (2013).
[7]K. Osberg, N. Schemm, S. Balkir, J. O. Brand, M. S. Hallbeck, P. A. Dowben, and M. W. Hoffman, IEEE Sens. J. **6**, 1531 (2006).
[8]J. Uher, S. Pospisil, V. Linhart, and M. Schieber, Appl. Phys. Lett. **90**, 124101 (2007).
[9]D. S. McGregor, T. C. Unruh, and W. J. McNeil, Nucl. Instrum. Methods Phys. Res., A **591**, 530 (2008).
[10]G. F. Knoll, *Radiation Detection and Measurement*, 4th ed. (John Wiley & Sons, 2010).
[11]O. Osberghaus, Z. Phys. **128**, 366 (1950).
[12]T. C. Doan, J. Li, J. Y. Lin, and H. X. Jiang, AIP Adv. **6**, 075213 (2016).
[13]T. C. Doan, S. Majety, S. Grenadier, J. Li, J. Y. Lin, and H. X. Jiang, Nucl. Instrum. Methods Phys. Res., A **783**, 121 (2015).
[14]T. C. Doan, S. Majety, S. Grenadier, J. Li, J. Y. Lin, and H. X. Jiang, Nucl. Instrum. Methods Phys. Res., A **748**, 84 (2014).
[15]J. Li, R. Dahal, S. Majety, J. Y. Lin, and H. X. Jiang, Nucl. Instrum. Methods Phys. Res., A **654**, 417 (2011).
[16]S. Grenadier, J. Li, J. Y. Lin, and H. X. Jiang, J. Vac. Sci. Technol., A **31**, 061517 (2013).
[17]S. J. Pearton, J. C. Zolper, R. J. Shul, and F. Ren, J. Appl. Phys. **86**, 1 (1999).
[18]D. V. Lang, in *Deep Centers in Semiconductors*, edited by S. T. Pantelides (Gordon and Breach, New York, 1986), p. 489.
[19]C. A. Klein, J. Appl. Phys. **39**, 2029 (1968).